ICAS 2020 SHANGHAI
International Council of the Aeronautical Sciences
32nd Congress of the International Council of the Aeronautical Sciences
September 6-10, 2021
Pudong Shangri-La, Shanghai, China

Experimental Study on the Characteristics of Sonic Gas Injection into Supersonic Crossflow with Ma2.0 and Ma3.0

Liang Changhai[1], Sun Mingbo[1,*], Yang Yixin[1], Liu Yuan[2], Wang Taiyu[1], Ma Guangwei[1], Li Fan[1] ,Wang Chao[1]

[1]Science and Technology on Scramjet Laboratory, College of Aerospace Science and Engineering, National University of Defense Technology, Changsha, 410073, China
[2]Science and Technology on Scramjet Laboratory, China Aerodynamics Research and Development Center, Mianyang, 621000, China

Abstract

The gaseous injection into a supersonic flow is one of the most fundamental methods of fuel mixing in scramjet engines. As the scramjet performs in a wide operating range of flight Mach number, the structure of the gaseous transverse jet flow also changes. This research combines NPLS (Nanoparticle-based Planar Laser Scattering) and oil flow experiments to study the flow structures of the transverse gaseous jet into a supersonic crossflow. The supersonic suction-type low turbulence wind tunnel of the National University of Defense Technology could provide inflow streams with different Mach numbers, including Ma2.0 and Ma3.0. We analyzed the instantaneous flow field structure by NPLS images and the near-wall friction characteristics by oil flow results, and compared the results with different dynamic pressure ratio under Ma2.0 and Ma3.0. Upstream the jet, the bow shocks under the inflow with Ma2.0 and the inflow with Ma3.0 vary significantly, especially the difference in shock angle. In the jet leeward, there is a V-shape separation zone. The characteristics of the separation zone under different conditions are analyzed. The results show that the bow shock angle and the separation angle are related to the inflow Mach number, but not to the jet dynamic pressure ratio *J*.

Keywords: transverse jet; supersonic crossflow; changing inflow Mach number; NPLS; oil flow

1. General Introduction

With the development of the aerospace industry, hypersonic propulsion has always been a concern of experts and scholars. Scramjet is the best choice for designing hypersonic aircraft propulsion system due to its excellent performance at high flying Mach number. Gaseous fuel injection mixing is a key sub-process of supersonic fuel organization. The efficient mixing of fuel and air is a necessary prerequisite for efficient engine combustion [1]. Transverse injection into a supersonic stream is one of the most fundamental canonical flows for supersonic propulsion community. As the scramjet engine performs in a wide range of speeds, the inflow Mach number of the scramjet differs and the gas fuel mixing characteristics differs.

The flow field has significant three-dimensional characteristics, including complex shock wave system, flow separation, recirculation and reattachment, wall free shear layer and other flow characteristics. The recent research progress of sonic transverse gas jet into a supersonic crossflow has been summarized in the research of Karagozian et al. [2] and Mahesh et al. [3].

Dickmann et al.[4] gave a detailed description of the impact of the shock wave-boundary layer on the jet flow. The typical flow topology of a sonic transverse jet from a wall surface into a supersonic flow

First author: liangchanghai123@163.com Tel: +86 13278875121
* Corresponding E-mail address: sunmingbo@nudt.edu.cn Tel:+86 13974807416
Third author: yangyixin@nudt.edu.cn Tel:+86 18229724060
Fourth author: yuanl1991@163.com Tel:+86 15281622026
Fifth author: 763844650@qq.com Tel:+86 15616016039
Sixth author: maguangwei_nudt@163.com Tel: +86 18374858464
Seven author: lifan_nudt@163.com Tel: +86 18373191630
Eighth author: businde@126.com Tel:+86 18773306681

is shown in Figure 1[4]. The jet flow field contains a complex three-dimensional a shock structure, a shear layer and their interaction. Upstream the jet, a bow shock wave is formed caused by the obstructive effect of the jet. The adverse pressure gradient generated by the obstructive effect of the jet would lead to the inflow boundary layer separation, which produces a separation shock. The separation shock and bow shock waves intersect, called "λ" shock system. The separation zone also induced a pair of horseshoe vortices. In our recent studies[5, 6], oil flow visualization clearly showed the near-wall characteristics of jet wakes, including the reflected shock, V-shape separation region and reattachment region. Besides, the barrel shock and Mach disk are presented.

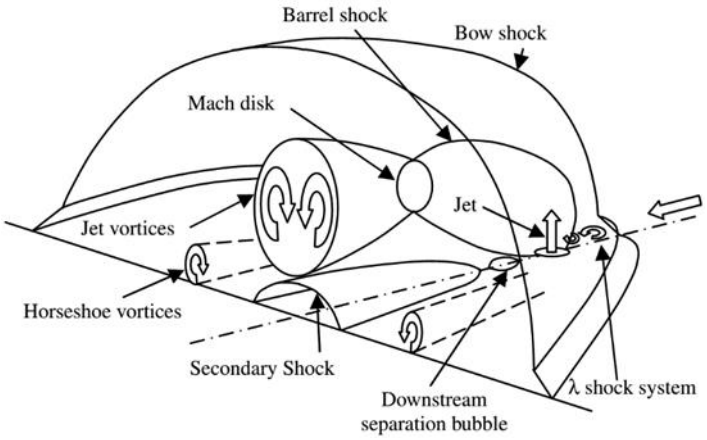

Figure 1 –3D view of near-field meanflow structure. [4]

New et al. [7] found that periodic leading edge vortices would be generated on the shear layer of the lateral inflow and jet plume. Kelso et al. [8] believed that such vortex structures were induced by K-H unstable vortices in the jet shear layer. Viti et al. [9] conducted the large eddy simulation to analyze the sonic transverse jet into a supersonic crossflow, which indicated the structure of the barrel shock and the Mach disk, and analyzed the development of vortex in the jet plume, as shown in Figure 2 and Figure 3[9]. Gruber[10] and Sun et al. [11] visualized the instantaneous structure of the flow field by experiments.

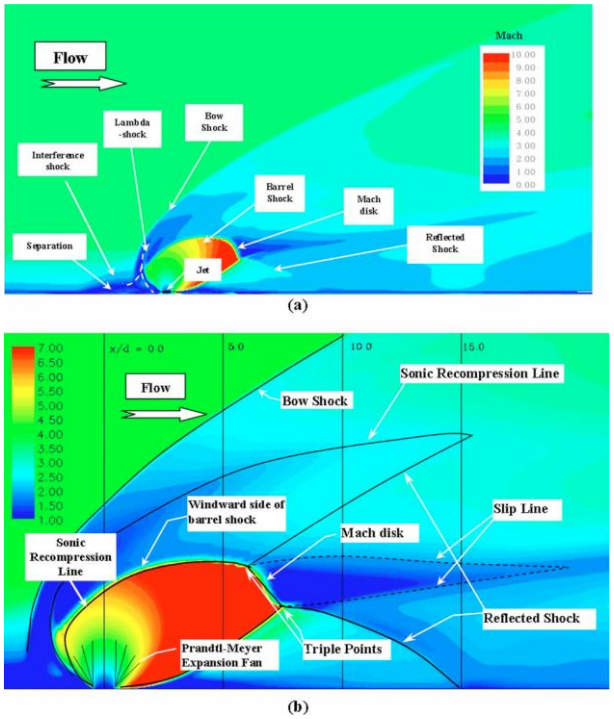

Figure 2 –Shock wave structures in the symmetrical slice. (*z/D*=0) [9]

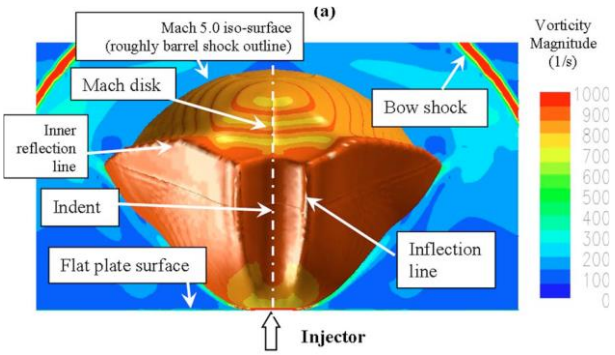

Figure 3-Barrel shock and Mach disk. [9]

Since the series of studies clarified a series of jet flow field characteristics and vortex development regulations. However, these studies are based on the constant incoming Mach number. For an actual scramjet, the inflow Mach number does not remain stable, such as changes in the vehicle's attitude, or acceleration process. It is quite valuable to study the variation of the transverse gas jet into a supersonic crossflow as inflow Mach number changes.

With the aim to study flow structures of the flow structures with supersonic crossflow of Ma2.0 and Ma3.0, this paper would give the detailed experimental techniques (the NPLS developed by Zhao et al.[19] and oil flow visualization) and detailed data analysis and discussion. This paper compared the characteristics of sonic gaseous injection into a supersonic crossflow with different Mach numbers (Ma2.0 and Ma3.0). The emphasis would be on the analysis of the flow field structure, especially the variation of the bow shock and the V-shape recirculation zone in the jet leeward.

2. Experimental descriptions

This experiment was conducted in a low-noise suction-type wind tunnel of the National University of Defense Technology. The schematic of the wind tunnel is given in Figure 4. A honeycomb screen is used to lower the free stream turbulent intensity. The nozzle is a Laval nozzle, which can accelerate the inflow air to supersonic speed and can be replaced according to different needs. In this paper, the nozzle of Ma2.0 and Ma3.0 are installed respectively. Nozzle and experimental section are integrated, which avoids shock waves caused by installation gaps. The exit of the wind tunnel is connected to a vacuum tank.

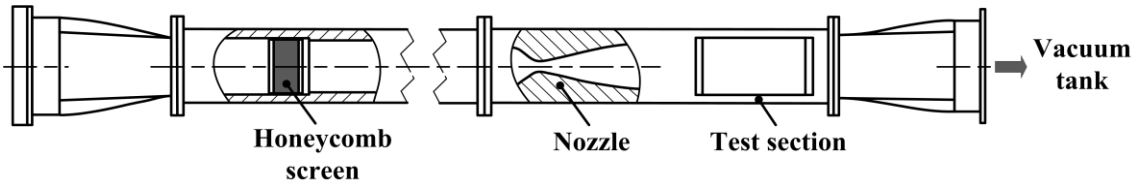

Figure 4-Schematic of the Low-Noise Wind Tunnel

Nanoparticle-based Planar Laser Scattering (NPLS) experiments were conducted to visualize the flow field on several slices, while oil flow techniques were employed to obtain the friction characteristics in the near wall region. The NPLS system consists of a IMPERX charge-couple device (CCD) camera, a double-pulsed Nd:YAG laser, a nanoparticle generator, a computer and a synchronizer. The Nd:YAG laser was operated at a wavelength of 532 nm, a pulse energy of 520mJ and a pulse width of 6 ns(±1 ns). The CCD camera and the laser were synchronized by a synchronizer with a controlling accuracy of 0.25 ns. Detailed descriptions about the experimental setups are illustrated in papers by Zhao et al.[12] and by Wang et al.[13]. The schematic of NPLS is shown in Figure 5.

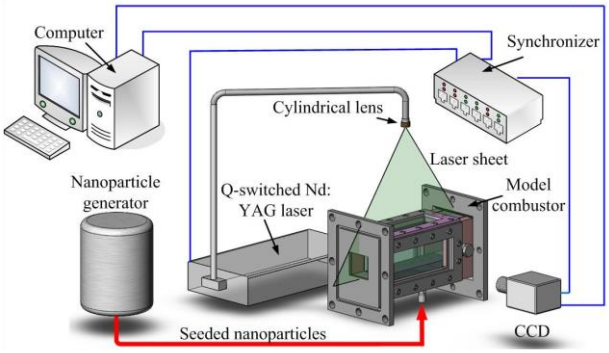

Figure 5- The schematic of NPLS. [12]

In the oil flow experiment, a special kind of oil is made into a pigment and spread evenly over the surface of the flat plat. The oil flow slowly and eventually forms skin-friction lines because of the viscous nature of the fluid near the wall in the experiment.

As shown in Table 1, the air inflow parameters are set in accordance with the Ma=3.0 and Ma=2.0 with stagnation pressure P_0 = 101325 Pa, stagnation temperature T_0=300 K. In the experiments, nitrogen is injected at a sonic velocity from a jet orifice with a diameter of D=2mm for all conditions. All cases lead to a sonic jet with stagnation temperature T_{0j}=300 K. The dynamic pressure ratio J is regarded as an important parameter that has a dominant effect on the jet penetration.

$$J = \rho_j V_j^2 / \rho_\infty U_\infty^2 \tag{1}$$

In this research, the dynamic pressure ratio J is chosen as 2.3, 5.5 and 7.7 respectively for Ma2.0 and Ma3.0 conditions. The detailed parameters are shown in Table 1.

Table 1 Air flow conditions and Nitrogen jet conditions for the experiments

Inflow Mach Number	Inflow Stagnation Temperature	Inflow Stagnation Pressure	Jet Orifice diameter D	Jet Mach number M_j	Jet Stagnation temperature T_{0j}	Jet-to-crossflow momentum J	Stagnation pressure P_{0j}
3.0	300K	101.325kPa	2mm	1	300K	2.3	226kPa
						5.5	539kPa
						7.7	755kPa
2.0						2.3	110kPa
						5.5	263kPa
						7.7	375 kPa

3. Results and Discussion

3.1 Experimental visualization of instantaneous transverse jet flow structures

Figure 6 and Figure 7 show NPLS images on the symmetry slice for Ma2.0 and Ma3.0 respectively. The instantaneous flow structures of the sonic jet into a supersonic crossflow are clearly distinguished for different dynamic pressure ratio J. From the symmetry slice, the bow shock and the inflow turbulent boundary layer upstream of the jet can be clearly observed. While the large-scale structures including K-H vortex and the highly turbulent wake structures dominate the downstream region. Nanoparticles shown in the wake structures come from the crossflow since nitrogen jet do not carry any nanoparticle. From the NPLS images, the angle of the bow shock wave upstream the

jet orifice under Ma2.0 condition is larger than that under Ma3.0 condition.

Upstream the jet, it is obvious that the λ shock has two feet standing in the inflow boundary layer. The λ shock feet function like a shock in front of blunt body, meaning that it is meaningless to study its shock angle in the near wall region. However, for dynamic pressure ratio *J*, the shock tail of the bow shock in the area away from the wall forms a fixed angle with the wall surface. Plenty of NPLS images show that the bow shock angle *α* keeps about 30.5° for *J*=2.3, while that keeps 31.7°for *J*=5.5, and 33.0° for *J*=7.7. It could be recognized that the bow shock angle keeps constant with the change of jet dynamic pressure ratio *J*.

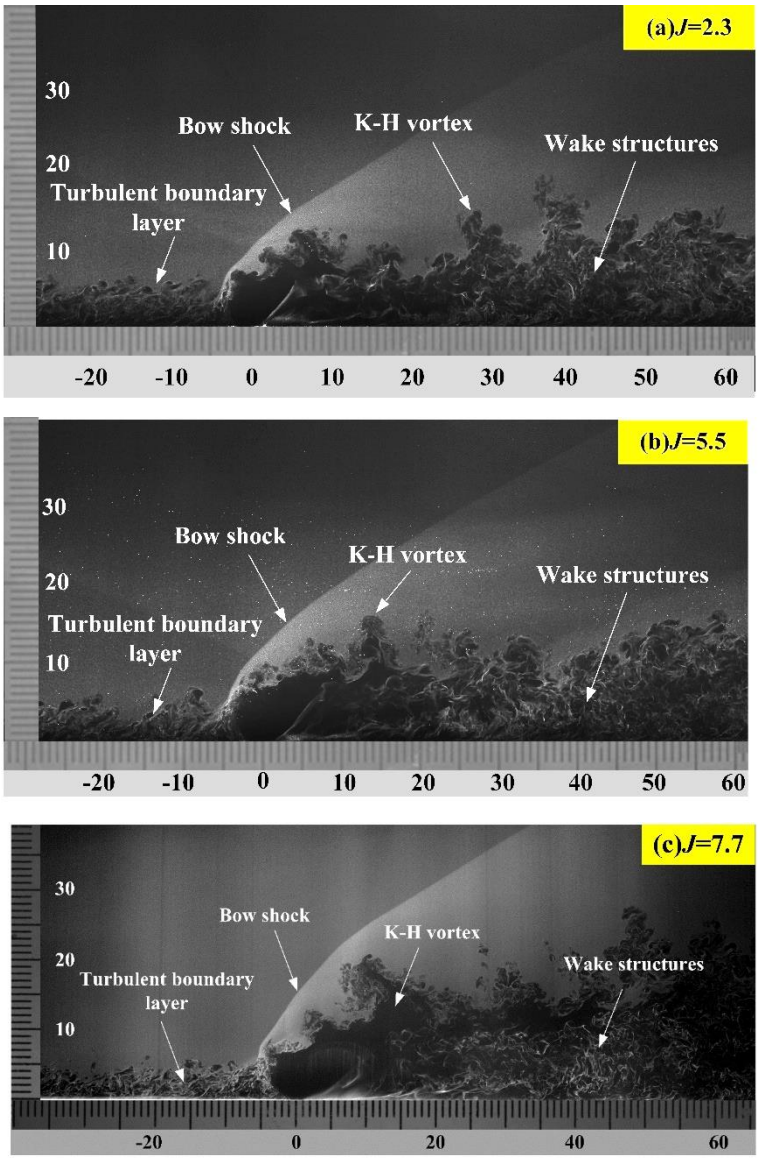

Figure 6 –Instantaneous streamwise flow structures at the symmetry (*z*=0mm) slice of *J*=2.3, 5.5 and 7.7 under Ma3.0 condition with *D*=2mm.

In the same way, the NPLS images for the inflow Mach number is Ma2.0 could be analyzed. As Figure 7 shows, the bow shock angle for Ma2.0 is much larger than that for Ma3.0. The bow shock angle keeps about 50.5° for *J*=2.3, while that keeps 51.6° for *J*=5.5, and 52.2° for *J*=7.7. The same conclusion could be drawn for Ma2, the bow shock angle does not change with dynamic pressure ratio *J*.

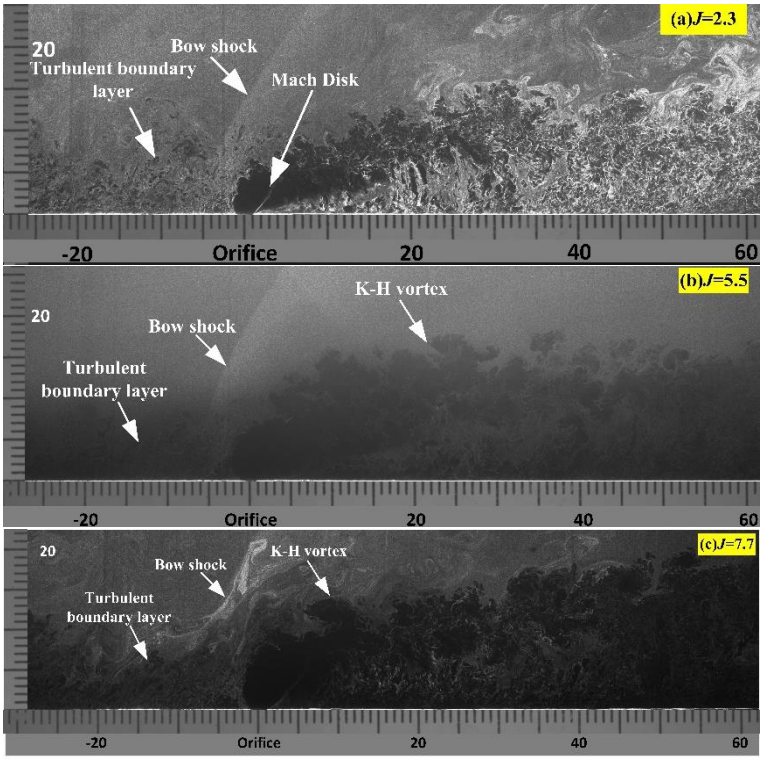

Figure 7-Instantaneous streamwise flow structures at the symmetry (z=0mm) slice under J=2.3, 5.5 and 7.7 and Ma2.0 condition with D=2mm.

In this paper, the angle formed by the projection of the bow shock on the symmetrical slice away from the wall area and the wall is defined as the bow shock angle. In general, the bow shock angle is related to the inflow Mach number, but not to the jet dynamic pressure ratio J. By numerical fitting of these data according to the relevant aerodynamic theory, the formula of the bow shock angle could be obtained

$$\alpha = 1.68 \times \arcsin\left(\frac{1}{Ma}\right) \tag{2}$$

Where α is the bow shock angle, the Ma is the inflow Mach number.

3.2 Near-wall friction characteristics by oil-flow experiments

Figure 8 and Figure 9 are oil flow images for Ma2.0 and Ma3.0 respectively, with different dynamic pressure ratio J. From these images, the skin-friction lines, the λ shock feet, the separation zone and the reattachment could be obviously distinguished. It is concluded in our previous work [5, 14, 15] that the V-shape separation region is induced by the V-shape collision shock. After the supersonic inflow bypasses the jet, it collides with each other on the jet leeward side to form a V-shaped collision shock. In the enlarged partially picture, it is clearly observed that the herringbone trailing feet stand in the jet leeward, showing the shape of the recirculation zone. In addition, other the skin-friction lines could reflects the interaction between the boundary layer and the wall. And the reflected shock could not be ignored.

The results showed that the angle of the V-shape recirculation zone are related to the Mach number of the crossflow rather than the jet-to-crossflow dynamic pressure flux ratio (J), and the angle under Ma2.0 condition is also larger than that under Ma3.0 condition. This conclusion has been reflected in our previous research [6], a comparison is given between J=7.7, 20.0 and J=28.9 cases. It is found that the recirculation angle θ is 34.2° for J=7.7, basically equal to that for J=20.0 (θ=34.5°) and J=28.9(θ=33.2°).

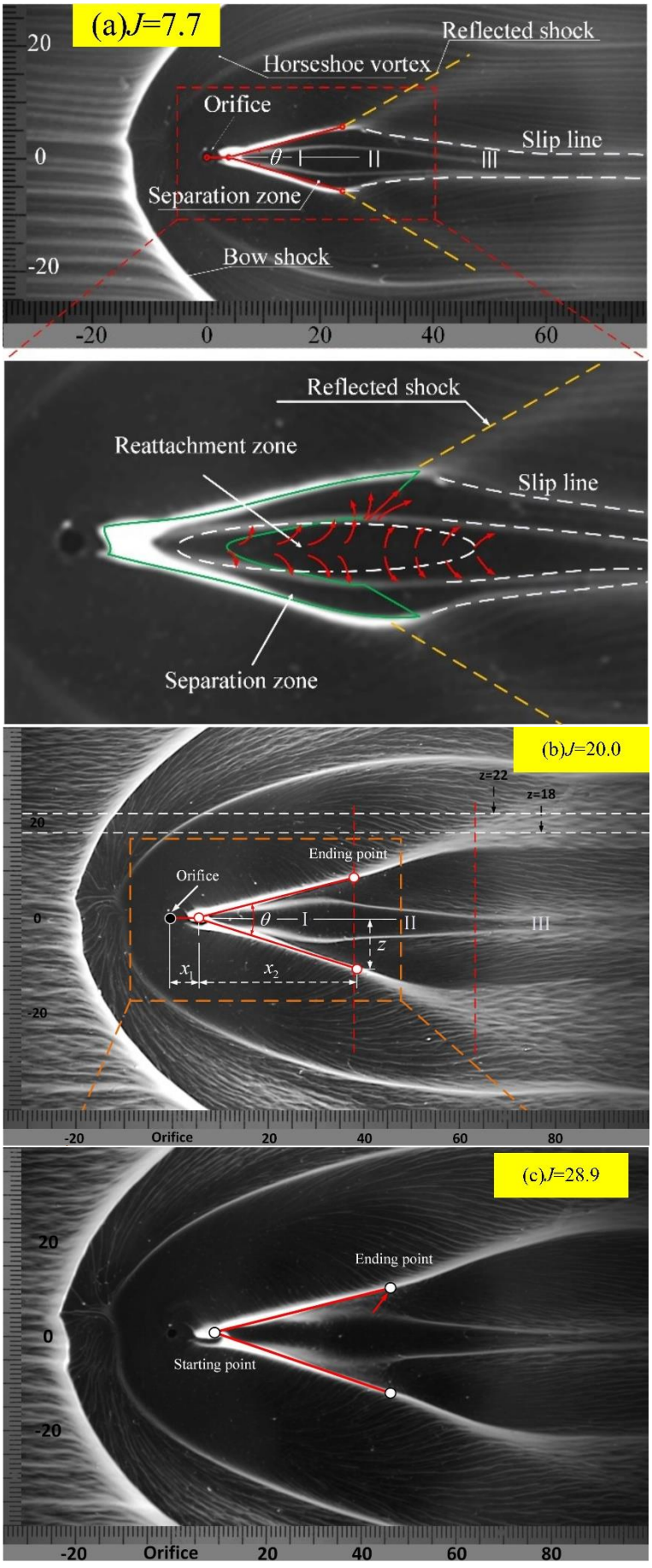

Figure 8 Skin-friction lines from experimental oil-flow pattern for (a)*J*=7.7, (b)*J*=20.0 and (c) *J*=28.9 under Ma3.0 condition[6].

Similarly, for the supersonic inflow of Ma2.0, it is found that the recirculation angle θ is 58.3° for J=5.5, basically equal to θ=60.5° for J=7.7. The same conclusion could be drawn for Ma2, the separation angle does not change with dynamic pressure ratio J.

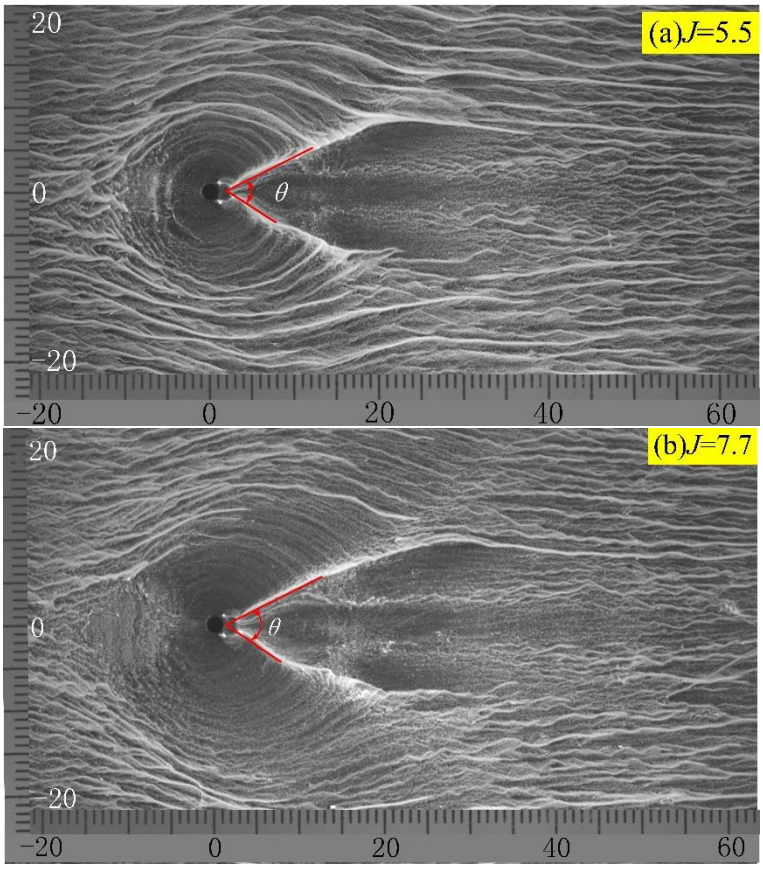

Figure 9- Skin-friction lines from experimental oil-flow pattern for (a)J=5.5 and (b)J=7.7 under Ma2.0 condition.

Similar to the analysis of the bow shock angle, the formula of the bow shock angle could be given

$$\theta = \eta \bullet \arcsin\left(\frac{1}{Ma}\right), \eta = 0.878 \tag{3}$$

Where θ is the bow shock angle, Ma is the inflow Mach number, η is the scaling factor.

4. Conclusions

In conclusions, both NPLS (Nanoparticle-based Planar Laser Scattering) technology and oil flow visualization are combined to study the flow structures of a transverse jet injected into a supersonic air crossflow of Ma=2.0 and Ma3.0. The experiments were carried out with the momentum flux ratio (J) of 2.3, 5.5 and 7.7. The main research conclusions can be listed as follows:

(1) The NPLS images shows that the instantaneous flow structures of Ma3.0 are similar with that of Ma2.0, including bow shock, K-H vortex, barrel shock and other interesting structures. The oil flow experiments could visualize the surface friction characteristics in the near- wall region. There is an obvious V-shape separation zone for all cases. Besides, λ shock and friction lines also could be observed in the near-wall region.

(2) In this paper, we define the bow shock angle as the angle between the bow shock on the symmetrical slice away from the wall area and the wall. By the analysis of NPLS images, Furthermore, the formula of the bow shock angle is given. It could be concluded that the bow shock angle is related to the inflow Mach number, but not to the jet dynamic pressure ratio J.

(3) In the near wall region, we compared the oil flow images under different conditions to study the angle of the V-shape recirculation zone in the jet leeward. The separation angle is defined as the angle between the two tails in the separation zone, and the formula of the separation angle is also added. The separation angle only depends on the Mach number of the crossflow rather than the jet-to-crossflow dynamic pressure flux ratio (J), and the angle under Ma2.0 condition is also larger than that under Ma3.0 condition. The formula of the separation angle is also added.

Acknowledgement

This work is funded by the National Science Foundation of China (grants: 11925207, 12002381 and 11802336).

Copyright Statement

References

[1] Huang W. Transverse jet in supersonic crossflows, Aerospace Science & Technology, 50, 183-195, 2016.

[2] Karagozian A R. Transverse jets and their control. Progress in Energy & Combustion Science, 36, 531-553,2010.

[3] Mahesh K. The Interaction of Jets with Crossflow. Annual Review of Fluid Mechanics, 45, 379-407,2013.

[4] Dickmann D A, Lu F K. Shock/boundary-layer interaction effects on transverse jets in crossflow over a flat plate. Journal of Spacecraft and Rockets, 46,1132-114, 2009.

[5] Liang C-h, Sun M-b, Liu Y, et al. Shock wave structures in the wake of sonic transverse jet into a supersonic crossflow. Acta Astronautica, 148,12-21, 2018.

[6] Liu Y, Sun M-b, Liang C-h, et al. Structures of near-wall wakes subjected to a sonic jet in a supersonic crossflow. Acta Astronautica, 151, 886-892, 2018.

[7] New T H, Lim T T, Luo S C. Elliptic jets in cross-flow. Journal of Fluid Mechanics, 494, 119-140,2003.

[8] Kelso R M, Lim T T, Perry A E. An experimental study of round jets in cross-flow. Journal of Fluid Mechanics, 306, 111-144,1996.

[9] Viti V, Neel R, Schetz J A. Schetz, Detailed flow physics of the supersonic jet interaction flow field. Physics of Fluids, 21, 296,2009.

[10] Gruber M R, Nejad A S, Chen T H, et al. Dutton, Large structure convection velocity measurements in compressible transverse injection flowfields. Experiments in Fluids, 22, 397-407,1997.

[11] Sun M B, Zhang S P, Zhao Y H, et al. Experimental investigation on transverse jet penetration into a supersonic turbulent crossflow. Science China Technological Sciences, 56, 1989-1998, 2013.

[12] Zhao Y X, Yi S H, Tian L F, et al. Supersonic flow imaging via nanoparticles, Science China Technological Sciences. 52, 3640-3648, 2009.

[13] Wang Q C, Wang Z G, Zhao Y X. On the impact of adverse pressure gradient on the supersonic turbulent boundary layer. Physics of Fluids (1994-present), 28,116101,2016.

[14] Sun M, Hu Z. Formation of surface trailing counter-rotating vortex pairs downstream of a sonic jet in a supersonic cross-flow. Journal of Fluid Mechanics, 850, 551-583, 2018.

[15] Liang C-h, Sun M-b, Wang Q-c, et al. Experimental study of parallel injections with different distances into a supersonic crossflow. Acta Astronautica, 168, 242-248, 2020.

Experimental Study on the Characteristics of Sonic Gas Injection into Supersonic Crossflow with Ma2 and Ma3